



Since January 2020 Elsevier has created a COVID-19 resource centre with free information in English and Mandarin on the novel coronavirus COVID-19. The COVID-19 resource centre is hosted on Elsevier Connect, the company's public news and information website.

Elsevier hereby grants permission to make all its COVID-19-related research that is available on the COVID-19 resource centre - including this research content - immediately available in PubMed Central and other publicly funded repositories, such as the WHO COVID database with rights for unrestricted research re-use and analyses in any form or by any means with acknowledgement of the original source. These permissions are granted for free by Elsevier for as long as the COVID-19 resource centre remains active.



ELSEVIER

Contents lists available at ScienceDirect

# Veterinary Microbiology

journal homepage: [www.elsevier.com/locate/vetmic](http://www.elsevier.com/locate/vetmic)

## Contribution of the porcine aminopeptidase N (CD13) receptor density to porcine epidemic diarrhea virus infection

Eeuri Nam, Changhee Lee \*

Department of Microbiology, College of Natural Sciences, Kyungpook National University, 1370 Sankyuk-dong, Buk-gu, Daegu 702-701, South Korea

### ARTICLE INFO

#### Article history:

Received 8 May 2009

Received in revised form 15 November 2009

Accepted 18 December 2009

#### Keywords:

Porcine epidemic diarrhea virus

Coronavirus

Porcine aminopeptidase N

Receptor density

APN enzymatic activity

### ABSTRACT

Porcine epidemic diarrhea virus (PEDV) and transmissible gastroenteritis virus (TGEV), which belong to group 1 coronaviruses, are important viral pathogens in pigs causing lethal diarrhea. As with the other members in the group 1, these viruses are also known to use the host aminopeptidase N (APN) as the major receptor for cell entry. Remarkably, it was found that they utilize distinct cultured cell lines for in vitro virus propagation, since PEDV could not be replicated in swine testis (ST) cells expressing native porcine APN (pAPN), which are highly susceptible to TGEV. To explain the mechanism causing this discrimination, we postulated that there may be a correlation between the pAPN expression level and PEDV infection. As a first step toward understanding the role of cellular receptor density in PEDV replication, therefore, sub-lines of ST cells stably overexpressing recombinant pAPN were generated. We initially confirmed that the control ST cells do express relatively low levels of endogenous pAPN. In contrast, in the engineered stable cell lines, a high level of recombinant pAPN expression was demonstrated. The introduction of a pAPN gene into nonpermissive ST cells was further found to be fully sufficient to support productive infection, revealing that constitutive overexpression of pAPN can directly rescue PEDV multiplication. We further assessed whether the pAPN enzymatic function is relevant to PEDV infection. The enzymatic active motif-null mutant pAPN still retained the ability to exert its receptor activity and consequently, to cause infectious virus production. Moreover, the only APN inhibitor blocking the protease activity site had no obvious negative effect on viral infection, indicating that the enzymatic role of APN is dispensable for the process of virus replication. Taken together, our results suggest that pAPN receptor density appears to be an important factor in contributing to efficient PEDV infection.

© 2009 Elsevier B.V. All rights reserved.

### 1. Introduction

The *Coronaviridae* family contains a diversity of important viral pathogens that can infect humans and animal species causing respiratory and gastroenteric diseases (Lai et al., 2007; Weiss and Navas-Martin, 2005). They are enveloped viruses possessing a single-stranded positive-sense approximately 30 kb RNA genome

with a 5' cap and a 3' polyadenylated tail (Lai et al., 2007). The virions are composed of a nucleocapsid (N) protein and three or four membrane-associated proteins, the peplomer or spike (S), membrane (M), hemagglutinin-esterase (HE), and a minor small envelope (E) proteins, present in a lipid-containing envelope (Lai et al., 2007). On the basis of serological and genotypic criteria, coronaviruses are divided into three distinct groups 1–3, which are members of the new order of *Nidovirales* together with the *Arteriviridae* family (Cavanagh, 1997; Spaan et al., 2005).

Coronaviruses have a limited host range and tissue tropism, which is determined by the interaction of the viral

\* Corresponding author. Tel.: +82 53 950 7365; fax: +82 53 955 5522.  
E-mail address: [changhee@knu.ac.kr](mailto:changhee@knu.ac.kr) (C. Lee).

S glycoprotein with a receptor protein on the surface of susceptible cells (Bosch et al., 2003; Gallagher and Buchmeier, 2001). A variety of cellular receptors for coronaviruses, which include carcinoembryonic antigen-related cell adhesion molecule 1 (CEACAM1), angiotensin-converting enzyme 2 (ACE2), and aminopeptidase N (APN), have been identified (Delmas et al., 1992; Li et al., 2003; Williams et al., 1991; Yeager et al., 1992). Most members in the group 1 coronavirus, human coronavirus-229E (HCoV-229E), feline infectious peritonitis (FIPV), canine coronavirus (CCoV), porcine epidemic diarrhea virus (PEDV), and transmissible gastroenteritis virus (TGEV), use the APN of their natural host species as a functional receptor for virus entry (Delmas et al., 1992; Kolb et al., 1998; Li et al., 2007; Tresnan et al., 1996; Yeager et al., 1992). APN, also known as CD13, is a 150-kDa type II glycoprotein that belongs to a membrane-bound metalloprotease family (Kenny and Maroux, 1982; Lendeckel et al., 2000; Look et al., 1989). The APN glycoprotein is predominantly expressed on the surface of epithelial cells of the kidney, small intestine, and respiratory tract, where the protein can be cleaved by trypsin into two N-terminal (95 kDa) and C-terminal (50 kDa) subunits (Kenny and Maroux, 1982; Lendeckel et al., 2000). In addition to its use as the major receptor for group 1 coronaviruses, APN serves as a zinc-dependent protease mediating the cleavage of the N-terminal amino acids from active peptides through the HELAH motif for enzymatic activity (Jongeneel et al., 1989; Lendeckel et al., 2000).

The swine-specific group 1 enteric coronaviruses, PEDV and TGEV, are antigenically distinguishable from each other (Lai et al., 2007; Pensaert and Yeo, 2006). Both viral pathogens commonly replicate in the differentiated enterocytes of the small intestine and accordingly, cause similar clinical symptoms with lethal watery diarrhea and dehydration in piglets (Pensaert and Yeo, 2006; Sanchez et al., 1992). Furthermore, they are both known to use porcine APN (pAPN) as a cellular receptor to gain virus entry (Delmas et al., 1992; Li et al., 2007). Despite using the same receptor, strikingly distinct cultured cell lines are employed for virus growth *in vitro*: PEDV could be adapted and cultivated in African green monkey kidney (Vero) cells but could not be grown in swine testis (ST) cells that weakly express native pAPN, while TGEV can be propagated in ST cells (Delmas et al., 1992; Hofmann and Wyler, 1988; Li et al., 2007). Although the mechanism underlying this notable discrepancy has not yet been deciphered, it is tempting to speculate that the expression level of pAPN may be involved in PEDV infection.

In this study, therefore, a panel of ST cells stably expressing recombinant pAPN was established to define the role of pAPN receptor level in PEDV infectivity. Overexpression of pAPN enabled nonpermissive ST cells to produce the infectious progeny virus. We also found that the APN inhibitor and mutations in the catalytic site of pAPN did not adversely affect overall virus replication, indicating that pAPN enzymatic activity was not involved in PEDV replication. Our study suggests that high pAPN receptor density may be a critical factor that contributes to favorable virus entry into the host cell leading the process of infection.

## 2. Materials and methods

### 2.1. Cells, virus, and antibodies

ST and Vero cells were cultured in alpha minimum essential medium ( $\alpha$ -MEM, Invitrogen) with 10% fetal bovine serum (FBS, Invitrogen) and antibiotic-antimycotic solutions (100 $\times$ ; Invitrogen). Human embryonic kidney (HEK-293T) cells were grown in Dulbecco's modified Eagle medium (DMEM) with high glucose (Invitrogen) supplemented with 10% FBS and antibiotic-antimycotic solutions. The cells were maintained at 37 °C with 5% CO<sub>2</sub>. A PEDV strain SM98-1 was obtained from the Korean National Veterinary Research and Quarantine Services and propagated in Vero cells as described previously (Hofmann and Wyler, 1988). The PEDV S glycoprotein-specific and N protein-specific monoclonal antibodies (MAbs) were kindly provided by Sang-Geon Yeo (Kyungpook National University, Daegu, South Korea). The polyclonal antibody recognizing pAPN obtained from BALB/c mice immunized with purified pAPN (Sigma) was a gift from Bang-Hun Hyun (National Veterinary Research and Quarantine Services, Anyang, South Korea).

### 2.2. Construction of the pAPN plasmids

DNA manipulation and cloning were performed according to standard procedures (Sambrook and Russell, 2001). The total RNA was extracted from the intestinal brush border membrane by using TRIzol Reagent (Invitrogen) and RT-PCR was used to amplify the full-length pAPN gene with the following primer pair: pAPN-Fwd (5'-CGAGCTCCCTTCTCACCTCAC-3') and pAPN-Rev (5'-GATGGACACATGCGGCATCTTG-3') or pAPN-Rev-His-tag (5'-CTATTAgatgatggtgatggtgGCTGTGCTCTATGAA-CC-3'), where lowercase letters represent six repetitive histidine codons. The PCR amplicons were individually cloned into pGEM-T Easy (Promega) and the resulting plasmids, pGEM-pAPN and pGEM-pAPN-His-tag, were sequenced in both directions using pGEM vector-specific primers. Each pAPN cDNA fragment obtained from pGEM-pAPN or pGEM-pAPN-His-tag was independently subcloned into a pFB-Neo retroviral vector (Stratagene), using a NotI restriction site to produce the pAPN expression plasmid pFB-Neo-pAPN or pFB-Neo-pAPN-His-tag. To modify the APN enzymatic motif (HELAH) at positions 383–387 in the pAPN protein, PCR-based site-directed mutagenesis was conducted to substitute the codons for histidine residues at positions 383 and 387 (genomic nucleotide positions 1146–1160) to codons for glutamine using pGEM-pAPN with the following mutagenic primer pair: H383/387Q-Fwd (5'-CTGTGATTGCTCAGGAGCTGG-CCCAGCAGTGGTTTGGC-3', nucleotide positions 1136–1173) and H383/387Q-Rev (5'-GCCAAACCACTGCTGGC-CAGCTCCTGAGCAATCACAG-3', nucleotide positions 1136–1173), where the underlined letters indicate codon changes for amino acid substitutions from 'HELAH' to 'QELAQ'. *E. coli* strains XL1-Blue (RBC) and DH5 $\alpha$  (RBC) were used as the hosts for site-directed mutagenesis and general cloning, respectively.

### 2.3. Generation of pAPN overexpressing stable cell lines

The retrovirus gene transfer system (Stratagene) was applied to generate a stable cell line expressing the recombinant pAPN gene. HEK 293T cells were co-transfected with three plasmids expressing the wild-type or mutant pAPN (pFB-Neo-pAPN, pFB-Neo-pAPN-His-tag or pFB-Neo-pAPN-H383/387Q), the Molony Murine Leukemia Virus (MMLV) *gag/pol* genes (pVPack-GP) and vesicular stomatitis virus (VSV) G protein (pVPack-VSV-G), respectively, for 48 h by using Lipofectamine 2000 (Invitrogen) according to the manufacturer's instructions to produce replication-defective retrovirus stocks. The retroviral culture supernatant was collected and used to infect target ST cells. Upon infection, the virus-infected target cells were allowed to be grown in the absence of a selectable marker. At 24 h post-infection, stable pAPN-expressing cells were selected with 1.5 mg/ml G418 (Invitrogen). Neomycin-resistant cell clones were examined by RT-PCR to determine the presence of the full-length pAPN gene, and the positive clones (ST-pAPN) were amplified for further analyses.

### 2.4. Immunofluorescence

To detect pAPN expression, the ST-pAPN cell lines were grown on microscope coverslips placed in 35-mm diameter dishes in  $\alpha$ -MEM containing 500  $\mu$ g/ml G418. At 48 h post-seeding, the cells were fixed with 4% paraformaldehyde for 10 min at room temperature (RT). The cells were blocked using 1% bovine serum albumin (BSA) in PBS for 30 min at RT and then incubated with polyclonal anti-pAPN antibody for 2 h. After washing five times in PBS, the cells were incubated for 1 h at room temperature with goat anti-mouse secondary antibody conjugated with Alexa Fluor 488 (Molecular Probes). For viral antigen detection, at 48 h post-infection, Vero or ST-pAPN cells inoculated with PEDV were fixed and permeabilized with 0.2% Triton X-100 in PBS at RT for 10 min. The virus-infected cells were then stained with N-specific Mab, followed by incubation with goat anti-mouse antibody conjugated with Alexa green. The cells were finally counterstained with 4',6-diamidino-2-phenylindole (DAPI, Sigma) and mounted on microscope glass slides in mounting buffer (60% glycerol and 0.1% sodium azide in PBS). Cell staining was visualized by a fluorescent Zeiss Axioplan 2 microscope (Carl Zeiss, Göttingen, Germany).

### 2.5. Fluorescence-activated cell sorting (FACS) analysis

The pAPN expression on the cell surface was analyzed by flow cytometry. Cells were trypsinized and centrifuged at  $250 \times g$  for 5 min. The cell pellet was washed with cold washing buffer (1% BSA and 0.1% sodium azide in PBS) and resuspended at  $1 \times 10^6$  cells in the primary anti-pAPN antibody or normal mouse IgG1 (Santa Cruz Biotechnology) diluted in 3% BSA-PBS. After incubation at 4 °C for 30 min, the cells were washed and incubated with Alexa Fluor 488-conjugated anti-mouse IgG secondary antibody diluted in 3% BSA-PBS at 4 °C for 30 min in the dark. The stained cells were washed again, fixed with 2%

formaldehyde solution, and analyzed using FACScan flow cytometry.

### 2.6. Immunoblots

ST or ST-pAPN cells grown in 6-well tissue culture plates for 48 h were solubilized in lysis buffer containing 0.5% Triton X-100, 60 mM  $\beta$ -glycerophosphate, 15 mM  $\rho$ -nitro phenyl phosphate, 25 mM MOPS, 15 mM,  $MgCl_2$ , 80 mM NaCl, 15 mM EGTA (pH 7.4), 1 mM sodium orthovanadate, 1  $\mu$ g/ml E64, 2  $\mu$ g/ml aprotinin, 1  $\mu$ g/ml leupeptin, and 1 mM PMSF for 30 min on ice and clarified by centrifugation at  $15,800 \times g$  (Eppendorf centrifuge 5415R) for 30 min at 4 °C. To detect the viral antigens, cell lysates were prepared from the PEDV-inoculated cells with a lysis buffer at 24 h post-infection. Protein concentrations of the cell lysates were determined by a BCA protein assay (Pierce). The cell lysates were mixed with  $4 \times$  NuPAGE sample buffer (Invitrogen) and boiled at 70 °C for 10 min. Proteins were separated on NuPAGE 4–12% gradient Bis-Tris gel (Invitrogen) under reducing conditions, and electrotransferred onto Immobilon-P (Millipore). The membranes were blocked with 3% powdered skim milk (Difco) in TBS (10 mM Tris-HCl [pH 8.0], 150 mM NaCl) with 0.05% Tween-20 (TBST) at 4 °C for 2 h, reacted at 4 °C overnight with the primary antibodies against pAPN, PEDV-N, -S, or  $\beta$ -actin (Santa Cruz Biotechnology). The blots were then incubated with horseradish peroxidase (HRP)-labeled goat anti-mouse IgG (Santa Cruz Biotechnology) at a dilution of 1:2000 for 2 h at 4 °C. Proteins were visualized by enhanced chemiluminescence (ECL) reagents (Amersham Biosciences) according to the instructions of the manufacturer.

### 2.7. PEDV infection in ST-pAPN cell lines

Vero or ST-pAPN cells were grown at  $5 \times 10^5$  cells/well in a 6-well tissue culture plate for 24 h. The cells were inoculated with PEDV at a multiplicity of infection (MOI) of 0.5 for 1 h at 37 °C. The virus inoculum was removed and the infected cells were maintained in fresh medium. To detect viral proteins, immunofluorescence and western blot analyses were conducted as described above. In order to identify PEDV, viral RNA was extracted from the lysates of the infected cells by using TRIzol (Invitrogen) and then used for RT-PCR to amplify the N gene with PEDV-N-Fwd (5'-GCCGGGATCCATGGCTTCTGTGACG-3') and PEDV-N-Rev (5'-GCCGGGATCCTTAATTTCTGTGTC-3'). Virus titers were determined by plaque assay as described previously (Lee et al., 2006) and plaques were stained with 1% crystal violet.

### 2.8. APN enzyme activity assay

The APN enzymatic activity in each cell line was determined as described previously (Ino et al., 1994). Briefly, ST or ST-pAPN cell lines were seed at  $5 \times 10^5$  in 60-mm diameter culture dishes and grown for 48 h at 37 °C. After washing with PBS, the cells were incubated in the presence of pre-warmed 1 mM L-leucine  $\rho$ -nitroanilide (Sigma) in 10 mM Tris buffer (pH 8.0) with 0.2 M KCl and

0.1 mM ZnSO<sub>4</sub> at 37 °C for 20 min. The reaction was terminated by adding three volumes of ice-cold PBS. The solution was harvested and clarified by centrifugation at 400 × g for 5 min at 4 °C and free  $\rho$ -nitroanilide in the supernatant was detected by absorbance measurement at 405 nm by a spectrophotometer (Mecasys). The assay was repeated three times and the error bars were determined by the standard deviation of the mean of the three replicates. Student's *t*-test was used for the statistical analysis and *p*-values of less than 0.05 were considered statistically significant.

### 2.9. The effect of APN inhibitors on PEDV infection

Stock solutions of bestatin, 2,2'-dipyridyl, and 1,10-phenanthroline (Sigma) were prepared in water at concentrations of 30, 25, and 15 mM, respectively, and further diluted to final concentrations as previously described (Yeager et al., 1992). ST-pAPN cells grown in 96-well plates were pre-incubated with various concentrations of APN inhibitors for 1 h and subsequently infected with PEDV at an MOI of 0.5 for 1 h at 37 °C in the presence or absence of the drugs. The virus inoculum was removed and the cells were washed three times with MEM. The inoculated cells were then incubated in fresh medium in the presence or absence of the reagents and monitored daily for the appearance of CPE. At 2 days post-infection, the ST-pAPN cells infected with PEDV in the presence or absence of the drugs were fixed with cold methanol and subjected to ABC immunoperoxidase staining by using a

Vectorstain ABC kit (Vector) to identify virus infectivity. In brief, the fixed cells were incubated with PEDV N-specific MAb. After washing, the cells were incubated with biotinylated anti-mouse IgG, followed by incubation with the avidin–biotin complex solution. The virus-infected cells were then stained with a peroxidase DAB substrate kit (Vector) according to the manufacturer's instructions.

## 3. Results

### 3.1. Generation of stable cell lines expressing pAPN

The pAPN protein serves as a functional receptor for both TGEV and PEDV. However, the cell culture system to propagate each virus is noticeably distinct in that attempts of PEDV infection in the porcine cells, including TGEV-susceptible ST cells, have been unsuccessful (Hofmann and Wyler, 1988). Thus far, our understanding of this observation is still poor, but the pAPN expression level on the surface of ST cells has been suggested to be involved in PEDV infection. In order to study the role of receptor density on PEDV infection, the sub-lines of ST cells were generated to overexpress wild-type recombinant pAPN or six histidine tagged-pAPN under the control of a retroviral LTR promoter. The established cell clones (ST-pAPN) were first subjected to RT-PCR to detect pAPN expression at the mRNA level followed by nucleotide sequencing. We failed to amplify the full-length native pAPN from normal ST cells, but were able to identify a pAPN gene of approximately 3 kb from the ST-pAPN cell clones (data not shown).

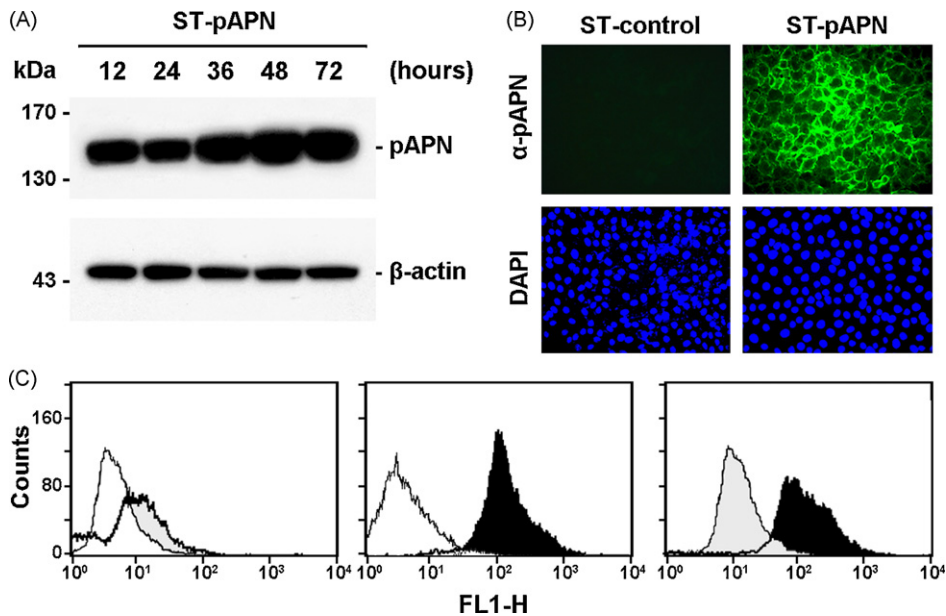


**Fig. 1.** Stable overexpression of the pAPN protein in ST-pAPN cells. (A) Immunoblot analysis of the pAPN protein. ST-pAPN cells were grown in a 6-well tissue culture plate at  $4 \times 10^5$  cells/well for 12, 24, 36, 48, and 72 h. Cell lysates were prepared at the indicated time points and subjected to western blot analysis with polyclonal anti-pAPN mouse antiserum to determine the expression level of the pAPN protein (upper panel). The blot was also reacted with mouse MAb against  $\beta$ -actin to confirm equal protein loading (lower panel). (B) Immunofluorescence assay of pAPN. ST or ST-pAPN cells were fixed with 4% formaldehyde at 2 days post-seeding and incubated with the pAPN-specific antiserum followed by goat anti-mouse secondary antibody conjugated with Alexa green (upper panels). The cells were then examined using a fluorescent microscope at 40× magnification. (C) Cell surface expression of pAPN. One million cells were incubated with anti-pAPN antiserum and analyzed by flow cytometry. In the flow cytometry panels, the white histogram indicates ST-pAPN cells stained with an isotype control, the gray histogram represent normal ST cells reacted with anti-pAPN antibody, and the black histogram shows ST-pAPN cells incubated with anti-pAPN antibody.

Next, pAPN expression at the protein level was confirmed by western blot and consequently, one ST-pAPN cell line that highly expressed pAPN was chosen for subsequent experiments. We identified the constitutive overexpression of the 150 kDa pAPN in ST-pAPN and its increased expression level with time, demonstrating high level expression and accumulation of pAPN (Fig. 1A). The ST-pAPN cell line was further examined for the cell surface expression of pAPN by FACS analysis and immunofluorescence. As with the previous study, the normal ST cells

exhibited minimal expression of the endogenous surface pAPN protein (Fig. 1C). In contrast, a significantly high level of pAPN expression on the plasma membrane was observed in ST-pAPN cells when compared to the control and even normal ST cells (Fig. 1C). Furthermore, the specific cell surface staining was clearly evident when ST-pAPN cells were incubated with the polyclonal anti-pAPN antibody without permeabilization, whereas no fluorescence was observed in normal ST cells, confirming the stable high-level surface expression of the pAPN protein

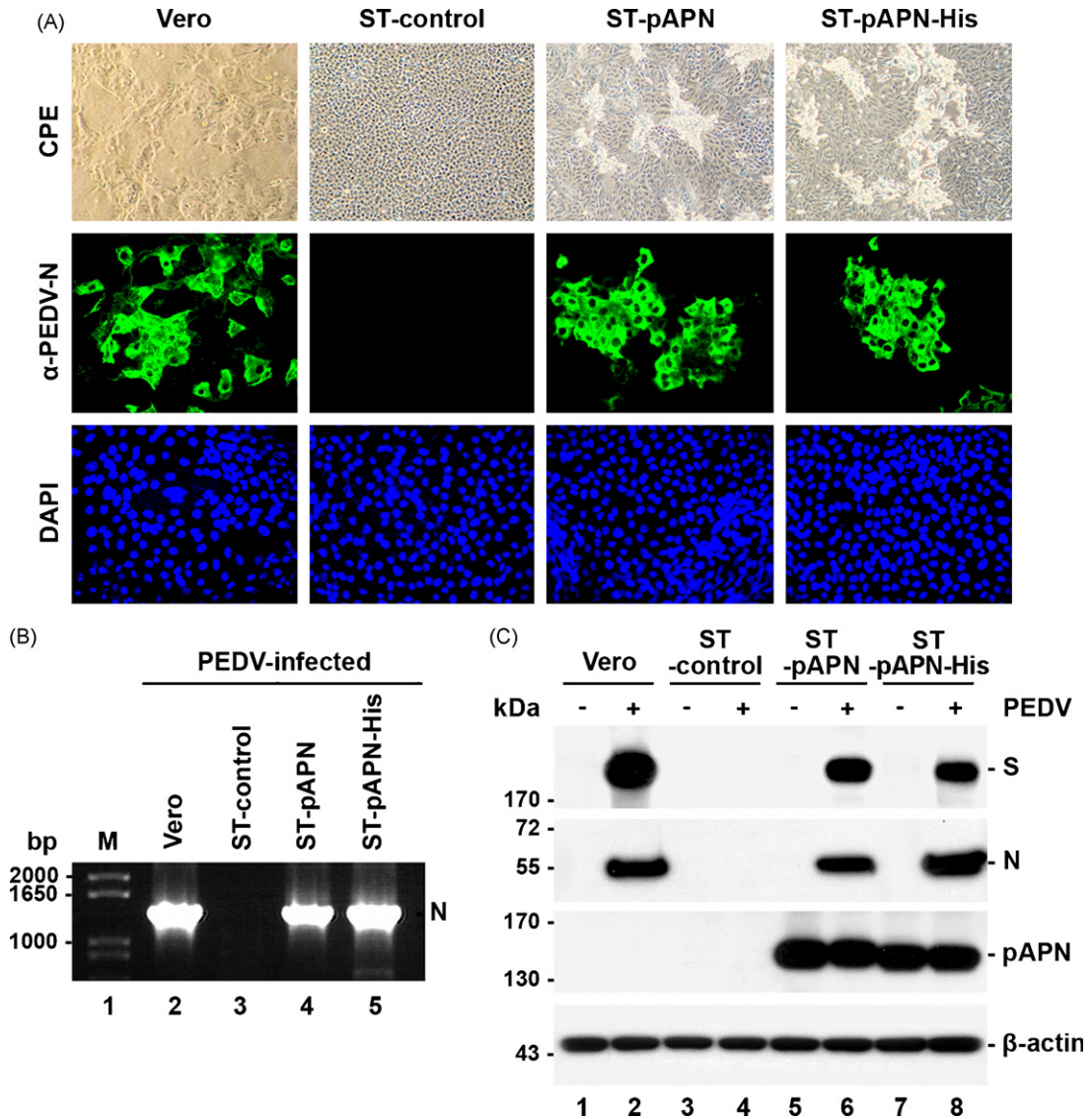


**Fig. 2.** Growth of PEDV on ST cells overexpressing pAPN. (A) PEDV infectivity in ST-pAPN cells. Individual cell lines were independently inoculated with PEDV at an MOI of 0.5 and further incubated for 3 days. PEDV-specific CPEs were observed daily and were photographed at 3 days post-infection using an inverted microscope at a magnification of 10× (upper panels). For immunostaining, infected cells were fixed at 2 days post-infection and incubated with the N-specific MAb followed by Alexa green-conjugated goat anti-mouse secondary antibody (middle panels). The cells were then counterstained with DAPI (lower panels) and examined using a fluorescent microscope at 40× magnification. (B) Detection of viral RNA by RT-PCR. Total RNA was extracted from cells inoculated with PEDV. A 1326-bp fragment corresponding to the PEDV N gene was RT-PCR amplified and visualized on a 0.8% agarose gel. Lane 1 (M), molecular weight marker; lane 2, infected Vero cells; lane 3, infected normal ST cells; lane 4, infected ST-pAPN cells; lane 5, infected ST-pAPN-His cells. (C) Identification of viral protein synthesis. Cell lysates were prepared from mock-infected or virus-infected cells at 24 h post-inoculation and immunoblotted to identify viral proteins with the PEDV S-specific (first panel) or N-specific MAb (second panel). The blot was also reacted with anti-pAPN (third panel) or anti-β-actin (fourth panel) antibodies to confirm the pAPN expression status or equal protein loading, respectively. Lanes 1, 3, 5, and 7, mock-infected cells; lanes 2, 4, 6, and 8, virus-infected cells.

(Fig. 1B). All the cells consistently showed specific fluorescent signals, indicating a homogenous population of cells expressing pAPN. In addition, the ST-pAPN-His cell lines stably expressing his-tagged recombinant pAPN were constructed to confirm the importance of the pAPN density for PEDV infection and subsequently, the high-level expression of the his-tagged protein was demonstrated by the same methods as described above with both anti-pAPN and anti-his tag antibodies (data not shown). We also created an ST cell line (ST-Neo) with the empty retroviral vector pFB-Neo and found the same expression property of pAPN that resulted in nonsusceptibility of ST-Neo cells to PEDV as confirmed in a normal ST cell line (data not shown). In subsequent studies, thus, the normal ST cells were used as a negative control.

### 3.2. Correlation between PEDV infection and receptor density

In order to understand the potential role of pAPN expression intensity in virus replication, the PEDV permissivity of ST cells stably overexpressing pAPN was assessed by monitoring the cytopathic effect (CPE) following infection. In normal ST cells, PEDV inoculation did not produce any visible CPE, confirming the absence of virus infectivity (Fig. 2A). In contrast, similar to virus-infected Vero cells, visible CPE appeared in ST-pAPN cells infected with PEDV at 2 days post-infection and became predominant by 3 days post-infection (Fig. 2A, upper panels). The specificity of CPE was confirmed by RT-PCR to amplify the PEDV N gene and by immunofluorescence using the N-specific MAb (Fig. 2A and B). At 2 days post-infection, N-specific staining was shown in many cell clusters indicating infection and the spread of the virus to the neighboring cells (Fig. 2A, middle panels). Next, virus infectivity was further demonstrated by western blot analysis. As shown in Fig. 2C, newly synthesized viral S and N proteins were clearly detected in PEDV-infected ST-pAPN cells (lane 6), indicating permissiveness to virus replication due to pAPN overexpression. The yield of the virus produced after PEDV infection in ST-pAPN cells was also assessed using the plaque assay. Upon PEDV infection, a typical titer was determined to be  $1.5\text{--}4 \times 10^4$  PFU/ml in

ST-pAPN cells. To obtain further evidence on the involvement of cellular receptor density in productive virus infection, we attempted to test PEDV infection in ST cells constitutively expressing the his-tagged recombinant pAPN (ST-pAPN-His). Likewise, the ST-pAPN-His cells were also demonstrated to be fully permissive to the growth of PEDV as evidenced by the detection of the viral genome and proteins (Fig. 2). In contrast, other stable ST cell lines that express low levels of pAPN showed inefficient virus production and peak viral titers did not exceed 100 PFU/ml in those cells that was more than 2 logs lower than those observed in ST-pAPN cell lines highly expressing pAPN. These results indicate that the density of pAPN is a critical factor for PEDV replication. Interestingly, while typical CPEs with syncytia formation due to cell fusions were observed in the infected Vero cells in the presence of trypsin, virus infection in stable ST-pAPN cell lines induced obviously distinct CPEs with accumulation of the lytic cells (Fig. 2A, upper panels). Taken together, our data demonstrated that exogenous introduction of recombinant pAPN truly makes non-permissive ST cells susceptible to PEDV infection.

### 3.3. Role of APN enzymatic activity in PEDV infection

Since APN acts as a zinc-dependent metalloprotease through the catalytic motif HExxH, it was of interest to determine whether the enzymatic function of APN is required for the overall process of infection. In order to address this question, we tried to construct the enzymatic site-null mutant pAPN (pAPN-H383/387Q) by using PCR-directed mutagenesis to change the two histidines of the motif HELAH to glutamines at amino acid positions 383 and 387 of pAPN. Using the resulting construct, an ST cell line stably expressing a mutated form of pAPN was established and named ST-pAPN-H/Q. To identify the mutant pAPN expression at the mRNA level, RT-PCR and nucleotide sequencing were conducted by using the generated ST-pAPN-H/Q cell clones. The results showed successful introduction of the mutated pAPN into ST cells (data not shown). Overexpression of the mutant pAPN-H383/387Q protein was further confirmed by western blot analysis with

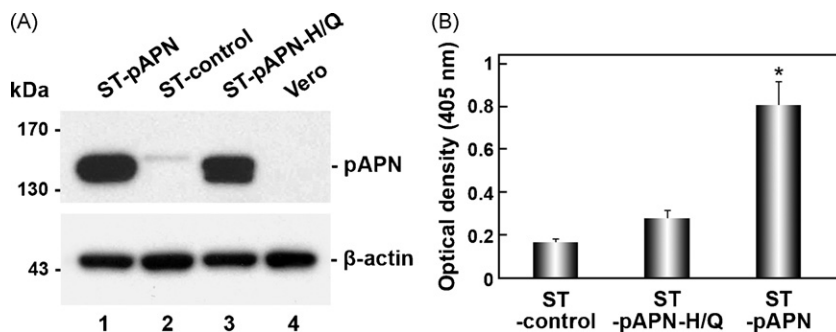


**Fig. 3.** Construction of a stable ST cell line expressing enzymatically defective mutant pAPN. (A) Expression of the catalytic motif-null pAPN protein. Western blot analysis was carried out using cell lysates prepared from the indicated cell line at 48 h post-seeding. The pAPN expression was detected using polyclonal anti-pAPN antiserum (upper panel). The bottom panel also shows  $\beta$ -actin expression to indicate equivalent loading. (B) Measurements of APN enzymatic activity. Each cell line was grown in 60-mm diameter culture dishes at  $5 \times 10^5$  for 48 h and then incubated with 1 mM L-leucine p-nitroanilide substrate buffer at 37 °C for 20 min. After centrifugation, the absorbance of the cell-free supernatants was measured at 405 nm by a spectrophotometer. These data are representative of three independent experiments and the error bars represent the mean standard deviation of the optical density values from the three replicates. \* $P=0.0005$  or  $0.00151$  compared with normal ST cells or ST-pAPN-H/Q cells, respectively.

polyclonal mouse antiserum to pAPN. As shown in Fig. 3A, the expression level of the mutated protein in ST-pAPN-H/Q cells was almost equal to the wild-type pAPN in ST-pAPN cells (lanes 1 and 3). The immunofluorescence assay further exhibited the strong cell surface signals of the enzymatic motif-null pAPN protein (data not shown). Thus, these data indicated that mutations in the enzymatic motif did not alter the expression density and the cellular localization of pAPN.

In order to confirm the expression of enzymatically defective pAPN in ST-pAPN-H/Q cells, the APN enzymatic activity test was performed (Fig. 3B). In the normal ST cells, because of small amounts of pAPN, the only basal level of the protease activity was observed. As expected, the ST-pAPN cells showed approximately four times more activity than the normal ST cells, indicating increased pAPN enzymatic function due to pAPN overexpression on the cell membrane. In contrast, cleavage reaction in ST-pAPN-H/Q cells was greatly reduced almost to the background level found in normal ST cells, thereby confirming that the proteolytic activity of the mutant pAPN-H383/387Q protein was significantly disrupted.

The receptor activity of enzymatically defective pAPN was then examined for virus infectivity by the infection of cells. ST-pAPN-H/Q cells were infected with PEDV, and the appearance of CPE was monitored daily. The virus induced visible CPE at 2 days post-infection in ST-pAPN-H/Q cells, indicating the production of the infectious progeny virus (Fig. 4A). PEDV-specific CPE was demonstrated by identifying the viral N gene from the virus-infected cells using RT-PCR (Fig. 4B). The synthesis of viral proteins was confirmed by immunofluorescence staining and western blot using N-specific MAb (Fig. 4A and C). In ST-pAPN-H/Q cells, clusters of cells showed bright fluorescence, indicating spread of the infectious virus (Fig. 4A). To further examine virus infectivity in ST-pAPN-H/Q cells, the yield of infectious virus was determined. A viral titer in ST-pAPN-H/Q cells was found to be similar to that obtained in ST-pAPN cells, producing indistinguishable plaque morphology (Fig. 4D, middle and lower panels). In contrast, no positive cells for virus infection were detected in the virus-infected ST cell control by using the methods described above (Fig. 4). Altogether, these results revealed that the

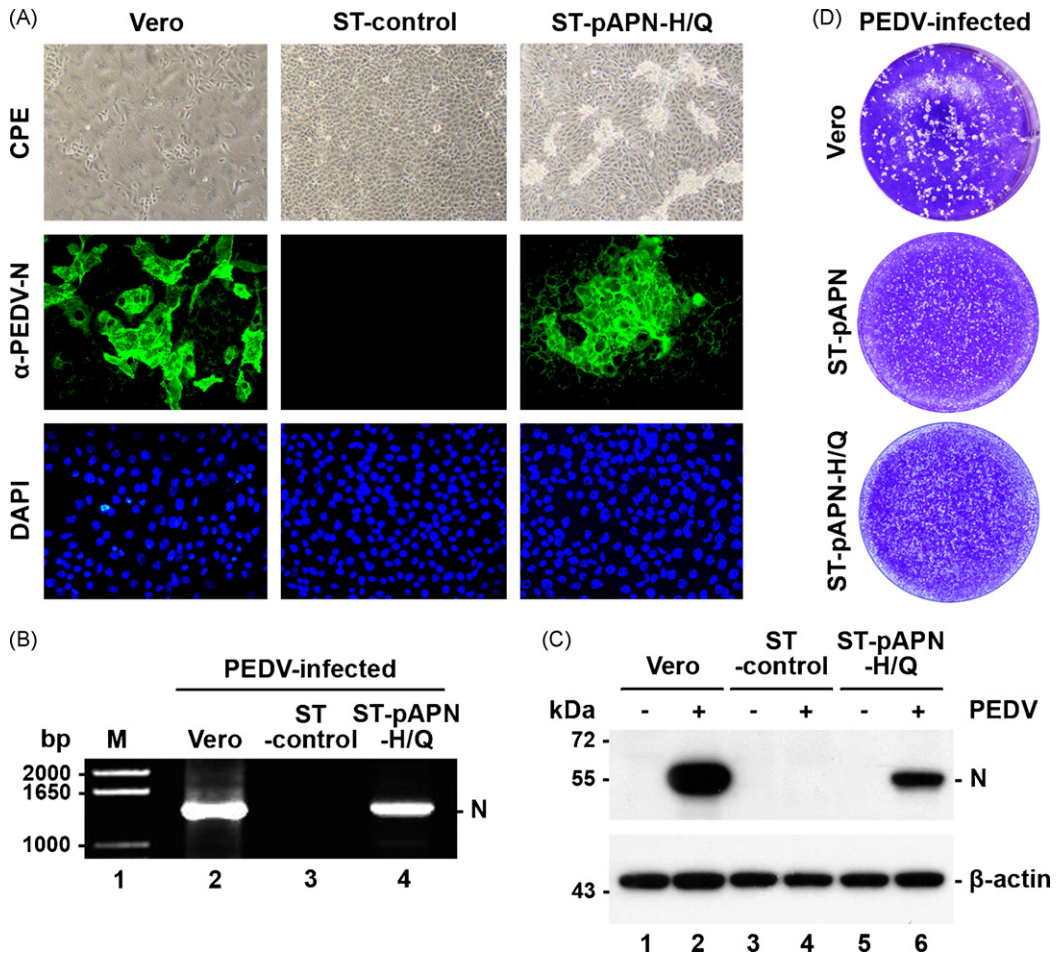


Fig. 4. Receptor activity of the mutant pAPN lacking the enzymatic activity. Vero, ST, or ST-pAPN-H/Q cells were separately inoculated with PEDV at an MOI of 0.5. The production of infectious progeny virus was determined by CPE appearance (A, upper panels), N-specific immunofluorescence staining (A, middle panels), RT-PCR (B), and western blot analysis with anti-N MAb (C). (D) Plaque morphology of PEDV in Vero, ST-pAPN, and ST-pAPN-H/Q cells. Upon infection, cells were overlaid with 0.8% agarose and incubated for 3 days. Plaques were stained with 1% crystal violet and photographed. Note that the size of plaques in PEDV-infected ST-pAPN-H/Q cells is indistinguishable from plaques in virus-infected ST-pAPN cells.



APN inhibitor	inhibition mode	Inhibition of PEDV infection
Bestatin	Enzymatic motif site	-
2,2'-Dipyridyl	Conformational change	+
1,10-Phenanthroline	Conformational change	+

**Fig. 5.** Effect of APN inhibitors on PEDV infection. The table summarizes the biological activities of APN inhibitors on virus replication. ST-pAPN cells were treated with bestatin (300  $\mu$ M) (B), 2,2'-dipyridyl (250  $\mu$ M) (C), and 1,10-phenanthroline (15  $\mu$ M) (D) for 1 h prior to PEDV infection and the virus-infected cells were further incubated for 2 days in the presence or absence of drugs. At 2 days post-infection, the cells were fixed with cold methanol and incubated with a PEDV N-specific MAb, followed by immunoperoxidase staining using Vectorstain ABC peroxidase and DAB substrate kits.

receptor activity of the mutant pAPN-H383/387Q remained unchanged.

To confirm the finding that the pAPN protease activity was irrelevant to virus infection, we investigated the effects of pAPN-specific inhibitors on PEDV replication. Non-involvement of the enzymatic activity during PEDV infection in ST-pAPN cells was thus assessed using three blockers of membrane-bound APN, bestatin, 2,2'-dipyridyl, and 1,10-phenanthroline. Bestatin is a small inhibitory molecule that binds competitively to the catalytic site of APN (Rich et al., 1984; Yeager et al., 1992). The remaining two inhibitors of APN activity, 2,2'-dipyridyl, and 1,10-phenanthroline, are known as zinc-chelating agents that alter the confirmation of the APN epitope, thereby preventing virus attachment (Vallee and Auld, 1990; Yeager et al., 1992). The inhibitory effect of individual compounds on virus replication was examined in the infected cells in the presence or absence of each blocker by immunoperoxidase staining using the N-specific MAb. As shown in Fig. 5A, efficient production of the infectious virus was again demonstrated in ST-pAPN cells infected with PEDV without drug treatment. In comparison to untreated infected cells, however, the number of N-specific staining-positive cells representing PEDV replication was dramatically reduced in cells treated with the drugs 2,2'-dipyridyl, and 1,10-phenanthroline, showing efficient inhibition of viral infection (Fig. 5C and D). In contrast, many clusters of PEDV-specific staining as seen in untreated infected cells were still retained in the bestatin-treated infected cells, suggesting no inhibitory effect of the drug on virus replication (Fig. 5B). Altogether, the data indicated that only the compound that effectively blocked the active site of APN was unable to display the ability to prevent virus production, demonstrating that APN enzymatic activity is non-essential for the process of infection.

#### 4. Discussion

The first step for successful virus entry and replication in the host is the recognition of the target cells through virus-receptor interactions. The presence of a specific

receptor(s) on the host cell surface is thus a major factor that determines the species specificity and tissue tropism of viruses. Although evolutionary diversities exist among different hosts or virus strains in the same virus family, employment of the viral receptor to enter the host cell seems to be selectively preserved. In contrast, members in the coronavirus family tend to show a variety of receptor usages depending on viral groups and species. Most group 1 coronaviruses use the host APN as a functional receptor to gain entry into cells (Delmas et al., 1992; Kolb et al., 1996; Tresnan et al., 1996; Yeager et al., 1992). HCoV-NL63 in group 1 and the severe acute respiratory syndrome coronavirus (SARS-CoV) in group 2 recognize human ACE2 to mediate virus entry (Hofmann et al., 2005; Li et al., 2003). In group 2 coronaviruses, mouse hepatitis virus (MHV) utilizes CEACAM1, whereas HCoV-OC43 and bovine coronavirus (BCoV) use N-acetyl-9-O-acetylneuraminic acid as a cellular receptor determinant (Williams et al., 1991; Schwegmann-Wessels and Herrler, 2006). Therefore, coronaviruses appear to adopt various strategies to recognize the appropriate receptor for attachment to the natural host.

The group 1 coronavirus contains two swine-specific enteropathogenic coronaviruses, TGEV and PEDV, which utilize pAPN as the major receptor for gaining virus entry. However, the cell culture system to support virus propagation is absolutely distinct since porcine cell lines including ST cells, which can be infected by TGEV, generally do not permit PEDV replication. The pAPN protein was originally identified as a functional receptor for TGEV in the ST cell extract, indicating pAPN expression in ST cells and thereby demonstrating the pAPN receptor usage of TGEV to enter ST cells (Delmas et al., 1992). Thus, because of the presence of pAPN on the ST cell surface, nonsusceptibility of ST cells to PEDV infection has been thought to be remarkably unusual. Since pAPN expression is known to be relatively weak in nonpermissive ST cells, one potent theory to explain such an observation that was applied in this study was that efficient virus replication seems to be associated with the expression level of pAPN on the cell surface. The current study was therefore conducted to investigate the role of the PEDV receptor

density in virus infection. To do so, stable cell lines overexpressing the recombinant pAPN protein were first established using ST cells, which express a low level of native pAPN. Our experiments showed that constitutive overexpression of pAPN is capable of rendering nonpermissive ST cells permissive to efficient PEDV infection. Furthermore, ST cell lines highly expressing pAPN mainly used in this study exhibited more efficient virus production compared with other cell lines that express relatively low levels of pAPN but higher levels than the normal ST cells. These data provide evidence that high pAPN receptor density beneficially contributes to the efficient production of infectious viruses. However, Delmas et al. (1995) have previously reported the contrary observations in the same cells infected with TGEV. The results of the previous study indicated that overexpression of pAPN in ST cells impairs the production of TGEV particles, whereas Madin–Darby canine kidney (MDCK) cells expressing low or large amount of pAPN fail to produce infectious particles. In contrast, the other study revealed that MDCK cells transiently expressing pAPN are capable of supporting PEDV infection (Li et al., 2007). Thus, it appears that the presence of other undetermined cell-specific factor(s) may reflect an inverse function of the pAPN expression level observed in TGEV-infected ST-APN cells. The characteristic CPE observed in Vero cells infected with PEDV in the presence of trypsin consists of vacuolation and formation of syncytia with up to 100 nuclei (Pensaert and Yeo, 2006). However, ST-pAPN cells infected with the virus produced cytopathology markedly distinguishable from that of infected Vero cells. Although the exact reason for this result remains undetermined, the striking difference in CPEs appears to be due to the induction of cell lysis by PEDV multiplication in specific cell type(s) such as ST cells in the absence of trypsin that became susceptible to virus infection by high-level expression of recombinant pAPN on their surface.

APN is a membrane-bound glycoprotein that acts as a zinc-binding protease (Look et al., 1989; Lendeckel et al., 2000). It is expressed on the epithelial cell surface of various tissues at different levels. More generally, APN is abundantly expressed in the brush border membrane of the small intestine and the kidney, whereas its expression is detected to a lesser extent in the liver, lung, and colon (Kenny and Maroux, 1982; Lendeckel et al., 2000). Remarkably, the aminopeptidase represents about 8% of the total protein content of the differentiated enterocytes in the small intestine mucosa (Delmas et al., 1992; Kenny and Maroux, 1982). As for natural PEDV infection, viral multiplication occurs in the cytoplasm of villous epithelial cells throughout the small intestine (Pensaert and Yeo, 2006). Moreover, the PEDV-induced histopathological lesions in piglets are only restricted to the small intestine (Pensaert and Yeo, 2006). The pathology of PEDV is thus noticeably consistent with the tissue distribution of pAPN. In the present study, the amounts of pAPN expressed in the established ST-pAPN cell lines are presumably similar to in vivo situation and consequently appear to be sufficient to lead to the growth of PEDV as with natural infection. It is also shown that in infected pigs, the site of TGEV multiplication is matched to tissues mainly distributing

the receptor, such as the small intestine. However, ST cells that minimally express pAPN are known to be fully permissive to the growth of TGEV in vitro. Unlike PEDV, therefore, TGEV infection seems to be much less confined by the pAPN receptor density at least in vitro. Nevertheless, in addition to the virus–receptor interactions, the receptor density on the plasma membrane of target cells could be another factor contributing to virus tropisms.

The pAPN protein possesses the enzymatic function that catalyzes the removal of amino acid residues from the N-terminals of oligopeptides (Jongeneel et al., 1989; Lendeckel et al., 2000). Another set of experiments was thus performed to examine whether the protease activity of pAPN is relevant to PEDV infection. We generated an ST cell line constitutively expressing the mutant pAPN, which was stripped of its enzyme activity by mutating the metalloprotease active motif. It was confirmed that the catalytic site mutation had no effects on the expression level and subcellular distribution of the pAPN protein. As with wild-type pAPN, the mutant enzyme activity-null pAPN was still able to retain the receptor activity. Furthermore, our data demonstrated that the only inhibitor blocking the APN active site was incapable of preventing PEDV replication, indicating that the proteolytic function of pAPN is non-relevant to the receptor activity in PEDV infection. This conclusion was somewhat expected since similar results have been obtained in previous studies with other coronaviruses, HCoV-229E and TGEV, which have also shown non-interference of the APN enzymatic activity in viral replication (Delmas et al., 1994; Yeager et al., 1992). Otherwise, it is interesting to note that small compounds inducing conformational changes in pAPN were found to be unfavorable to mediate virus entry. This finding further implicates the potential usefulness of these drugs as antiviral agents to treat acute PED infection.

In the present study, we cannot rule out a possible mechanism to explain the growth of PEDV on the monkey kidney-derived Vero cells. Shibata et al. (2000) have showed that PEDV is able to efficiently replicate in cultured cells directly prepared from the porcine kidney, where high pAPN density has been reported. Given the strict host tropism of PEDV for pigs, however, it has been unexpected that the virus could infect the monkey kidney cells. It is noteworthy that this cell line also permits replication of SARS-CoV through the specific binding of the viral S protein to the receptor molecule ACE2 on Vero cells (Ksiazek et al., 2003; Li et al., 2003). It is unclear if monkey APN (mAPN) is expressed in Vero cells and can be used as a functional receptor for PEDV infection. Although feline APN (fAPN) has been known to serve as a receptor for several group 1 coronavirus, the interaction between their S protein and the pAPN receptor generally acts in a species-specific manner (Tresnan et al., 1996; Wentworth and Holmes, 2001). For example, pAPN serves as a receptor for the porcine coronaviruses but not for HCoV-229E and vice versa (Delmas et al., 1994; Kolb et al., 1996). Furthermore, pAPN has only 78% amino acid identity to mAPN with the introduction of five gaps, whereas human APN (hAPN) shares 96% similarity to mAPN with one deletion residue. It is therefore unlikely possible that the PEDV S protein can recognize mAPN on Vero cells to gain virus entry. Rather, it

hints at the presence of additional factors such as unidentified receptors or receptor-independent infection that may contribute to the permissiveness of Vero cells to PEDV infection.

In conclusion, the data presented here showed that high pAPN receptor density has a pivotal role in determining PEDV entry for a subsequent multiplication cycle. Additionally, the current study revealed that the function of pAPN as a protease is irrespective of the process of PEDV infection. From this observation, we deduced that the molecular determinants necessary for the PEDV–receptor interaction appear to reside within a pAPN domain distinct from the catalytic site. However, more detailed studies are needed to dissect pAPN domains in order to determine the specific region that binds to the S protein during the PEDV–pAPN interaction. An alternative approach can be devised to construct a truncated soluble form of pAPN that may also interfere with viral replication. Finally, the insights obtained from this work will facilitate identification of the receptor-binding domain (RBD) of the PEDV S protein that can induce potent neutralizing antibodies. These next tasks will undoubtedly provide promising data to enable the development of antiviral agents and an effective and safe subunit vaccine for the prevention of PEDV infection.

### Acknowledgment

This work was supported by National Research Foundation of Korea Grant funded by the Korean Government (MEST) (KRF-2007-313-E00525).

### References

- Bosch, B.J., van der Zee, R., de Haan, C.A., Roitter, P.J., 2003. The coronavirus spike protein is a class I virus fusion protein: structural and functional characterization of the fusion core complex. *J. Virol.* 77, 8801–8811.
- Cavanagh, D., 1997. Nidovirales, a new order comprising Coronaviridae and Arteriviridae. *Arch. Virol.* 142, 629–633.
- Delmas, B., Gelfi, J., L'Haridon, R., Vogel, L.K., Sjöstrom, H., Noren, O., Laude, H., 1992. Aminopeptidase N is a major receptor for the enteropathogenic coronavirus TGEV. *Nature* 357, 417–420.
- Delmas, B., Gelfi, J., Kut, E., Sjöstrom, H., Noren, O., Laude, H., 1994. Determinants essential for the transmissible gastroenteritis virus–receptor interaction reside within a domain of aminopeptidase-N that is distinct from the enzymatic site. *J. Virol.* 68, 5216–5224.
- Delmas, B., Kut, E., Gelfi, J., Laude, H., 1995. Overexpression of TGEV cell receptor impairs the production of virus particles. *Adv. Exp. Med. Biol.* 380, 379–385.
- Gallagher, T.M., Buchmeier, M.J., 2001. Coronavirus spike proteins in viral entry and pathogenesis. *Virology* 279, 371–374.
- Hofmann, H., Pyrc, K., van der Hoek, L., Geier, M., Berkhout, B., Pöhlmann, S., 2005. Human coronavirus NL63 employs the severe acute respiratory syndrome coronavirus receptor for cellular entry. *Proc. Natl. Acad. Sci. U.S.A.* 102, 7988–7993.
- Hofmann, M., Wyler, R., 1988. Propagation of the virus of porcine epidemic diarrhea in cell culture. *J. Clin. Microbiol.* 26, 2235–2239.
- Ino, K., Goto, S., Okamoto, T., Nomura, S., Nawa, A., Isabe, K., Tomoda, Y., 1994. Expression of aminopeptidase N on human choriocarcinoma cells and cell growth suppression by the inhibition of aminopeptidase N activity. *Jpn. J. Cancer Res.* 85, 927–933.
- Jongeneel, C.V., Bouvier, J., Bairoch, A., 1989. A unique signature identifies a family of zinc-dependent metalloproteases. *FEBS Lett.* 267, 289–294.
- Kenny, A.J., Maroux, S., 1982. Topology of microvillar membrane hydrolyses of kidney and intestine. *Physiol. Rev.* 62, 91–128.
- Kolb, A.F., Maile, J., Heister, A., Siddell, S.G., 1996. Characterization of functional domains in the human coronavirus HCV 229E receptor. *J. Gen. Virol.* 77, 2515–2521.
- Kolb, A.F., Hegyi, A., Maile, J., Heister, A., Hagemann, M., Siddell, S.G., 1998. Molecular analysis of the coronavirus–receptor function of aminopeptidase N. *Adv. Exp. Med. Biol.* 440, 61–67.
- Ksiazek, T.G., Erdman, D., Goldsmith, C.S., Zaki, S.R., Peret, T., Emery, S., Tong, S., Urbani, C., Comer, J.A., Lim, W., Rollin, P.E., Dowell, S.F., Ling, A.E., Humphrey, C.D., Shieh, W.J., Guarner, J., Paddock, C.D., Rota, P., Fields, B., DeRisi, J., Yang, J.Y., Cox, N., Hughes, J.M., LeDuc, J.W., Bellini, W.J., Anderson, L.J., 2003. A novel coronavirus associated with severe acute respiratory syndrome. *N. Engl. J. Med.* 348, 1953–1966.
- Lai, M.C., Perlman, S., Anderson, L.J., 2007. Coronaviridae. In: Knipe, D.M., Howley, P.M., Griffin, D.E., Martin, M.A., Lamb, R.A., Roizman, B., Straus, S.E. (Eds.), *Fields Virology*. Lippincott Williams & Wilkins, Philadelphia, pp. 1305–1336.
- Lee, C., Hodgins, D., Calvert, J.G., Welch, S.W., Jolie, R., Yoo, D., 2006. Mutations with the nuclear localization signal of the porcine reproductive and respiratory syndrome virus nucleocapsid protein attenuate virus replication. *Virology* 346, 238–250.
- Lendeckel, U., Kähne, T., Riemann, D., Neubert, K., Arndt, M., Reinhold, D., 2000. Review: the role of membrane peptidases in immune functions. *Adv. Exp. Med. Biol.* 477, 1–24.
- Li, B.X., Ge, J.W., Li, Y.J., 2007. Porcine aminopeptidase N is a functional receptor for the PEDV coronavirus. *Virology* 365, 166–172.
- Li, W., Moore, M.J., Vasilieva, N., Sui, J., Wong, S.K., Berne, M.A., Somasundaran, M., Sullivan, J.L., Luzuriaga, K., Greenough, T.C., Choe, H., Farzan, M., 2003. Angiotensin-converting enzyme 2 is a functional receptor for the SARS coronavirus. *Nature* 426, 450–454.
- Look, A.T., Ashmun, R.A., Shapiro, L.H., Peiper, S.C., 1989. Human myeloid plasma membrane glycoprotein (gp150) is identical to aminopeptidase N. *J. Clin. Investig.* 83, 1299–1307.
- Pensaert, M.B., Yeo, S.G., 2006. Porcine epidemic diarrhea. In: Straw, B.E., Zimmerman, J.J., D'Allaire, S., Taylor, D.J. (Eds.), *Diseases of Swine*. Wiley-Blackwell, Ames, pp. 367–372.
- Rich, D.H., Moon, B.J., Harbeson, S., 1984. Inhibition of aminopeptidases by amastatin and bestatin derivatives. Effect of inhibitor structure on slow-binding processes. *J. Med. Chem.* 27, 417–422.
- Sambrook, J., Russell, D.W., 2001. *Molecular Cloning: A Laboratory Manual*, third ed. Cold Spring Harbor Laboratory Press, Cold Spring Harbor, NY.
- Sanchez, C., Gebauer, M.F., Sune, C., Mendez, A., Dopazo, J., Enjuanes, L., 1992. Genetic evolution and tropism of transmissible gastroenteritis coronavirus. *Virology* 190, 92–105.
- Schwegmann-Wessels, C., Herrler, G., 2006. Sialic acids as receptor determinants for coronaviruses. *Glycoconj. J.* 23, 51–58.
- Shibata, I., Tsuda, T., Mori, M., Ono, M., Sueyoshi, M., Uruno, K., 2000. Isolation of porcine epidemic diarrhea virus in porcine cell cultures and experimental infection of pigs of different ages. *Vet. Microbiol.* 72, 173–182.
- Spaan, W.J.M., Brian, D., Cavanagh, D., de Groot, R.J., Enjuanes, L., Gorbalenya, A.E., Holmes, K.V., Masters, P.S., Rottier, P.J., Taguchi, F., Talbot, P., 2005. Family Coronaviridae. In: Fauquet, C.M., Mayo, M.A., Maniloff, J., Desselberg, U., Ball, L.A. (Eds.), *Virus Taxonomy: Eighth Report of the International Committee on Taxonomy of Viruses*. Elsevier Academic Press, London, pp. 947–964.
- Tresnan, D.B., Levis, R., Holmes, K.V., 1996. Feline aminopeptidase N serves as a receptor for feline, canine, porcine, and human coronaviruses in serogroup I. *J. Virol.* 70, 8669–8674.
- Vallee, B.L., Auld, D.S., 1990. Zinc coordination, function, and structure of zinc enzymes and other proteins. *Biochemistry* 29, 5647–5659.
- Weiss, S.R., Navas-Martin, S., 2005. Coronavirus pathogenesis and the emerging pathogen severe acute respiratory syndrome coronavirus. *Microbiol. Mol. Biol. Rev.* 69, 635–664.
- Wentworth, D.E., Holmes, K.V., 2001. Molecular determinants of species specificity in the coronavirus receptor aminopeptidase N (CD13): influence of N-linked glycosylation. *J. Virol.* 75, 9741–9752.
- Williams, R.K., Jiang, G.S., Holmes, K.V., 1991. Receptor for mouse hepatitis virus is a member of the carcinoembryonic antigen family of glycoprotein. *Proc. Natl. Acad. Sci. U.S.A.* 88, 5533–5536.
- Yeager, C.L., Ashmun, R.A., Williams, R.K., Cardellicchio, C.B., Shapiro, L.H., Look, A.T., Holmes, K.V., 1992. Human aminopeptidase N is a receptor for human coronavirus 229E. *Nature* 357, 420–422.